Solar-Terrestrial Physics. 2024. Vol. 10. Iss. 3. P. 58–65. DOI: 10.12737/stp-103202407. © 2024 O.V. Sapunova, N.L. Borodkova, G.N. Zastenker. Published by INFRA-M Academic Publishing House

UDC 523.62-726
DOI: 10.12737/stp-103202407

Received March 29, 2024
Accepted May 13, 2024

SPECTRAL PROPERTIES OF SOLAR WIND PLASMA FLUX AND MAGNETIC FIELD FLUCTUATIONS ACROSS FAST REVERSE INTERPLANETARY SHOCKS

O.V. Sapunova
Space Research Institute RAS,
Moscow, Russia, sapunova_olga@cosmos.ru

G.N. Zastenker
Space Research Institute RAS,
Moscow, Russia, gzastenk@iki.rssi.ru

N.L. Borodkova
Space Research Institute RAS,
Moscow, Russia, nlbor@mail.ru

Abstract. We have analyzed spectra of fluctuations in the solar wind plasma flux and the magnetic field magnitude near the front of fast reverse shocks, using data from the BMSW device (Bright Monitor of Solar Wind) operating on the SPEKTR-R satellite. Its time resolution made it possible to study plasma flux fluctuations up to a frequency of 16 Hz. Magnetic field data was taken mainly from the WIND satellite, for which the frequency of the fluctuations considered was up to 5.5 Hz.

The slope of the spectra of the solar wind flux fluctuations on MHD scales has been shown to be close to the slope of the spectrum of magnetic field fluctuations in the disturbed region. On kinetic scales, the difference can be significant. For the region ahead of the front, the difference in the slope of the spectrum can be quite large both in the MHD and in the kinetic region.

The frequency of the break of the flux spectrum ranges from 0.6 to 1.3 Hz, which corresponds to the scale of the proton inertial length. In a number of events, however, the shape of the spectrum indicates the influence of the proton gyroradius frequency, which is usually 0.05–0.15 Hz. The break in the power spectrum of magnetic field fluctuations also more often ranges from 0.7 to 1.2 Hz. In this case, the slope of the MHD part of the spectrum changes little, but in the kinetic part it increases slightly when moving to the disturbed region.

Keywords: solar wind, interplanetary shocks, fluctuations.

INTRODUCTION

The solar wind (SW) is a natural laboratory for studying plasma turbulence [Bruno, Carbone, 2013; Kolmogorov, 1962; Leamon et al., 2000]. It is believed that in SW the energy of the system is contained in structures with scales more than 10^6 km and is transferred to smaller scales through a cascade of turbulent fluctuations. Kinetic processes begin to play an important role on scales of the order of proton gyroradius (~10^3 km), energy dissipation and hence plasma heating occur [Matthaeus et al., 2016]. Special attention should be paid to the change in plasma turbulence at the intersection of magnetohydrodynamic (MHD) discontinuities, such as interplanetary (IP) shocks, which are formed during a nonlinear increase in the wave steepness and can be divided (Figure 1) into fast forward (FF), fast reverse (FR), slow forward (SF) and slow reverse (SR) [Oliveira, 2017]. Sources of IP shocks of first two types are usually coronal mass ejections and compression regions at the boundary of slow and fast SW. Waves at the leading edge of the magnetic cloud and the compression region will be forward (FF); and at the trailing edge, reverse (FR), propagating toward the Sun [Pitňa et al., 2021].

When large-scale plasma turbulence (on scales larger than the ion gyroradius) develops due to the passage of FF-type IP shocks, its power increases, and the power spectral density (PSD) is similar for downstream and upstream SW regions [Pitňa et al., 2021]. Similar results indicating that the power of magnetic field fluctuations increases

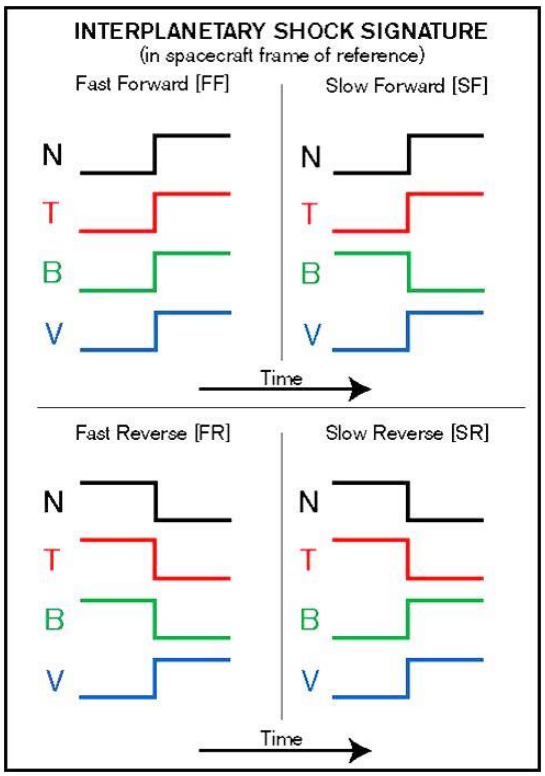

Figure 1. Types of interplanetary shocks and their associated behavior of plasma density (*N*), temperature (*T*), magnetic field (*B*), and solar wind velocity (*V*); variations of the parameters are presented according to the time of recording by the spacecraft

during the transition from upstream to downstream SW regions when crossing the front of fast forward IP shocks are presented in [Zhao et al., 2021]. Shocks of other types are studied much less frequently [Park et al., 2023].

To identify differences between the shock types, we have expanded the statistics to include fast forward and fast reverse shocks in the study. We have calculated coefficients of the slope of fluctuation power spectrum in both downstream and upstream SW regions from magnetic field and plasma flux data separately for the MHD spectral region and the transition region.

Turbulence has been examined using BMSW plasma flux data in [Šafránková et al., 2015, 2016]. One of the parameters considered was the position of the spectrum break, which shows the transition from MHD scales to kinetic ones and is determined by the processes responsible for energy dissipation in plasma. Depending on which process prevails and is the leading for a given set of parameters, the position of the break may correspond, for instance, to the proton inertial length L (fluctuations are conditioned by the transfer of energy between thin current sheets [Leamon et al., 2000; Smith et al., 2001]) or the proton gyroradius R (the fluctuations stem from a cascade of Alfvén fluctuations [Howes et al., 2008; Schekochihin et al., 2009]). The frequency determined by the ion inertial length:

$$F_L = V/2\pi L, \qquad (1)$$

where V is the plasma flux velocity; $L = s/\omega_i$ is the ion inertial length, $\omega_i=(4\pi n_i/m_i)^{1/2}$ is the ion plasma frequency.

We have divided the fluctuation spectrum at the frequency corresponding to the proton inertial length. The frequency related to the proton gyroradius is, however, indicated too.

1. DATA AND PROCESSING TECHNIQUE

We have used data from BMSW (Bright Monitor of Solar Wind) of the SPEKTR-R satellite [Zastenker et al., 2013; Šafránková et al., 2013]. In 2011–2019, 55 fast forward and 14 fast reverse IP shocks were recorded. The proton velocity, temperature, and proton and ion densities were determined for all the events, and proton flux and magnetic field fluctuation spectra were constructed. The interplanetary magnetic field magnitude and components were obtained from WIND data. The shock propagation velocity V_{IP} was determined by a geometric method from four satellites' data.

Recording of a fast forward IP shock is exemplified in Figure 2. At 14:19:05 UT on July 14, 2014, the SPEKTR-R satellite detected a jump in the SW plasma parameters.

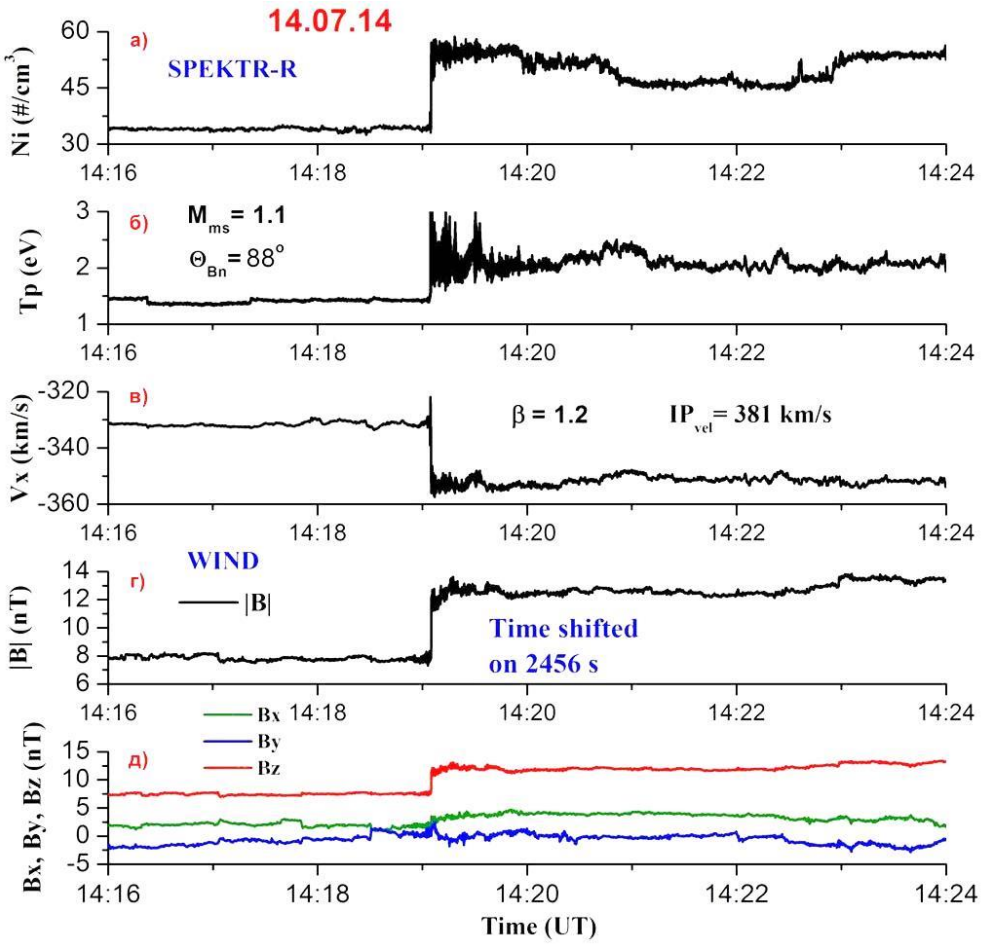

Figure 2. Time variation during the passage of fast forward IP shock on July 14, 2014: ion densities (*a*); proton temperatures (*b*); plasma flux velocity V_x (*c*); IMF magnitude (*d*); IMF components (in GSE coordinates) (*e*). For the magnetic field magnitude and components, the time is shifted by 2456 s to synchronize with the SPEKTR-R satellite

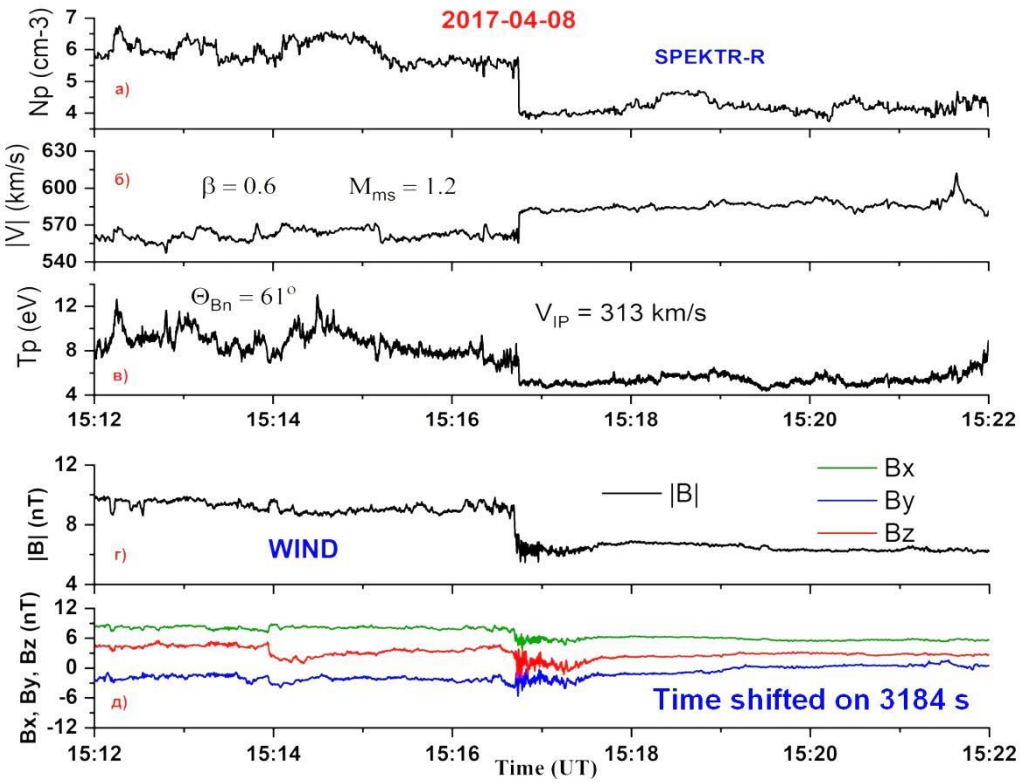

Figure 3. Time variation during the passage of fast reverse IP shock on April 08, 2017: proton density (*a*); plasma flux velocity (*b*); proton temperature (*c*); IMF magnitude (*d*); IMF component (in GSE coordinates) (*e*). For the magnetic field magnitude and components, the time is shifted by 3184 s to synchronize with the SPEKTR-R satellite

In the upstream region, the ion density was ~37 cm^{-3}; the proton temperature, ~1.5 eV, and the plasma flux velocity V_x=–332 km/s (in GSE coordinates). The IMF magnitude was 8 nT, with B_z making the main contribution. After passing the IP shock front, the density increased approximately twice, to 54 cm^{-3}, and the temperature reached 2 eV (apart from fluctuations immediately behind the front, where the temperature might have been as high as 2.5 eV). The velocity jump was low and amounted to ~26 km/s, which is below the mean for such events. The magnetic field magnitude increased 1.5 times — to 12 nT. All parameters increased when crossing the IP shock front.

A different pattern is observed during the passage of a fast reverse shock. Referring to Figure 1, in the case of a reverse shock all the parameters decrease except for the SW velocity. Such an event is illustrated in Figure 3.

The event, we classified as a reverse shock, was recorded on April 08, 2017 at 15:16:44 UT. The SW proton density decreased from 6.7 to 4 cm^{-3}; the temperature, from 7 to 5 eV, whereas the flux velocity rose from 546 to 583 km/s. The magnetic field magnitude also decreased from 10 to 6 nT, with B_x making the main contribution to this event. The reverse shock propagation velocity V_{IP} was 313 km/s, which is lower than the velocity of the forward shock recorded on July 14, 2014 (381 km/s). The parameter β (the ratio of gas pressure to magnetic pressure) for FR appeared to be two times lower than that for FF — 1.2. The magnetosonic Mach number M_{ms} was small for both events — 1.2 for FR and 1.1 for FF.

To construct the fluctuation spectra, we took 40 min intervals before/after crossing of the shock front, with a 5 min offset from the ramp, in order to exclude the influence of the fine structure (overshoot, undershoot, wave trains). The parameter of interest was normalized to the mean for this interval.

2. RESULTS

2.1. Statistics on variations in solar wind and classifying parameters

The statistics on variations in plasma and magnetic field parameters, as well as classifying parameters, are presented in Figures 4 and 5. Figure 4 shows that the mean change in the IMF magnitude for reverse IP shocks is less, even if insignificantly, than for forward ones. The difference in density change is more pronounced — in forward IP shocks it can increase fourfold, but for reverse IP shocks we did not have a case with N_d/N_u>3. The statistics on variations in the two remaining parameters — temperature and jump in the transport solar wind velocity — seems much more interesting. In reverse IP shocks, the temperature rose a maximum of two times; whereas in forward IP shocks, more than six times. The jump in transport velocity for forward IP shocks could exceed 200 km/s, and for reverse IP shocks it exceeded 120 km/s in only two events.

Figure 5 presents the statistics of classifying IP shock parameters. It is possible to observe some similarity in the parameter β for IP shocks of both types — for most events with β≤2, although there were a sufficient number of events in the sample for which β ranged from 2 to 4. The distributions of the angle θ_{Bn} between the direction of the magnetic field vector at the pre-front and the normal to

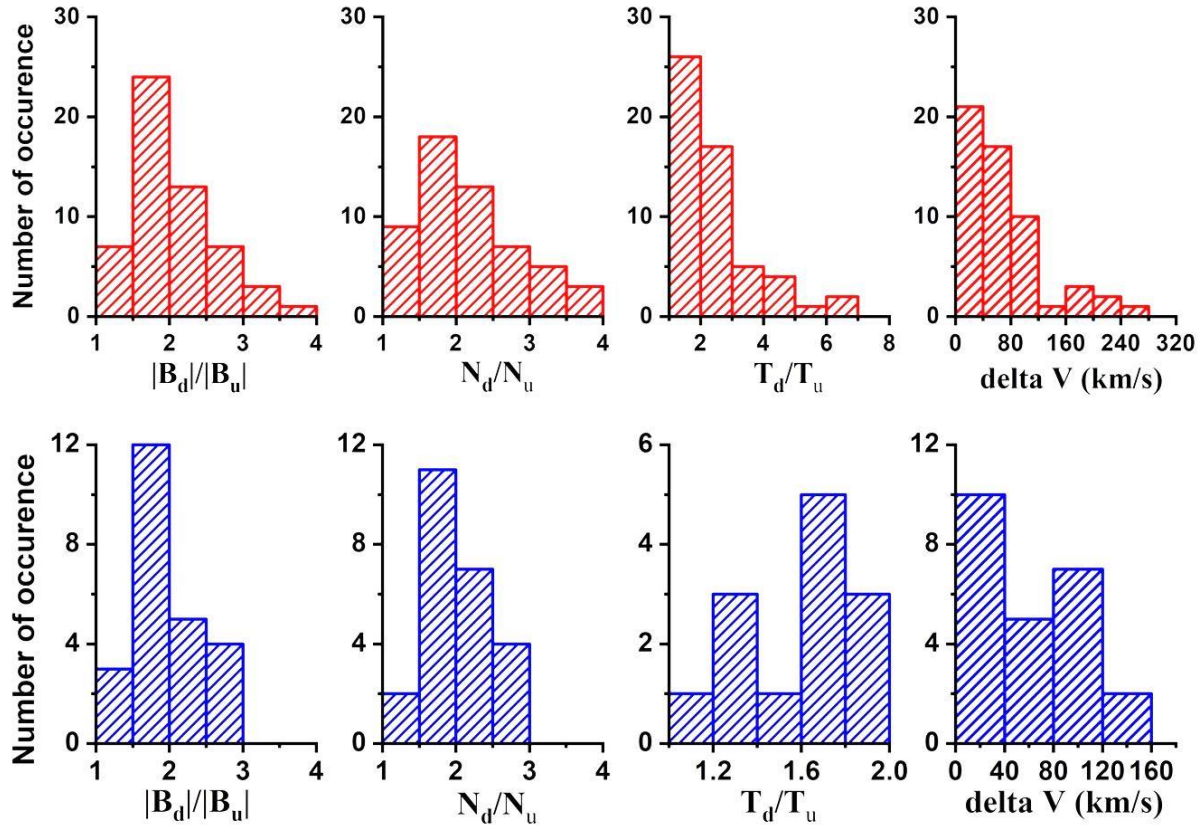

Figure 4. Variation in SW plasma parameters during the passage of FF (red) and FR (blue) IP shocks. The u and d indices indicate upstream and downstream solar wind regions

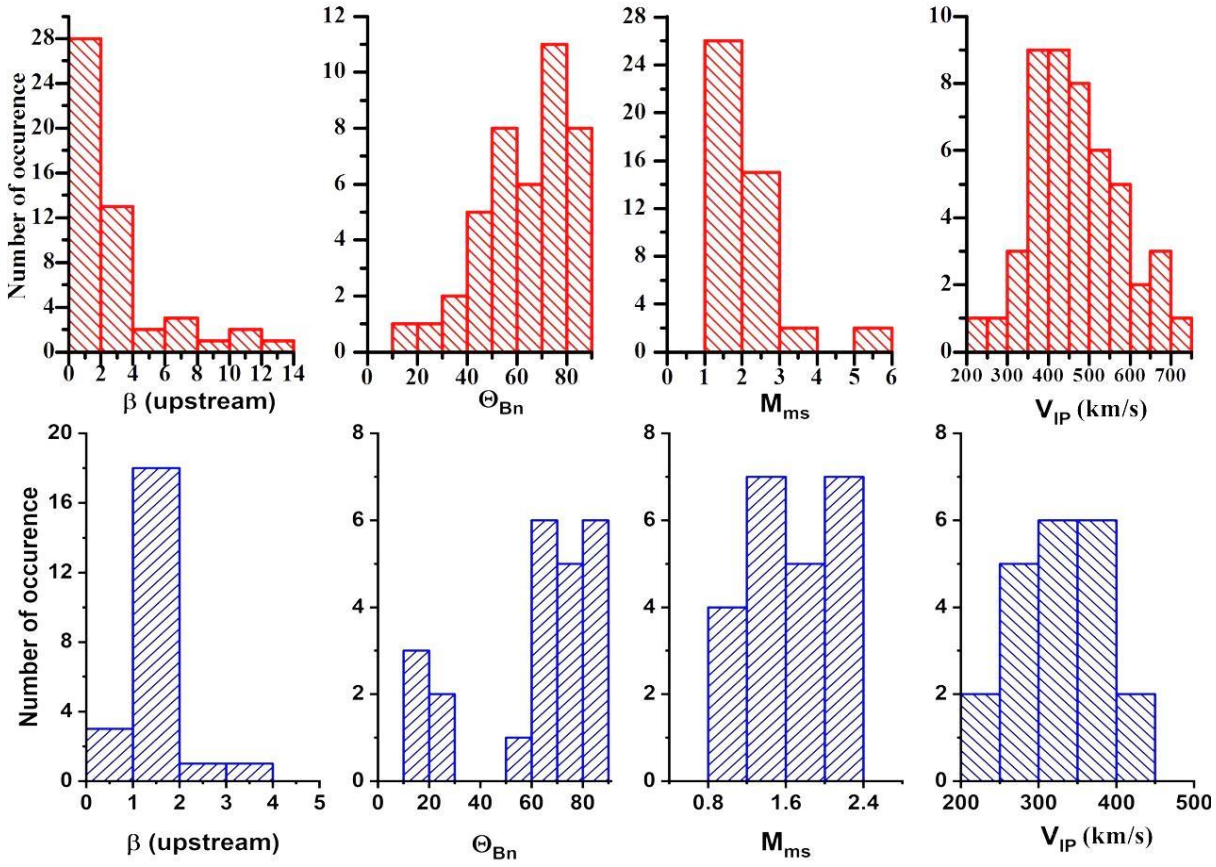

Figure 5. Classifying plasma parameters of FF (red) and FR (blue) IP shocks

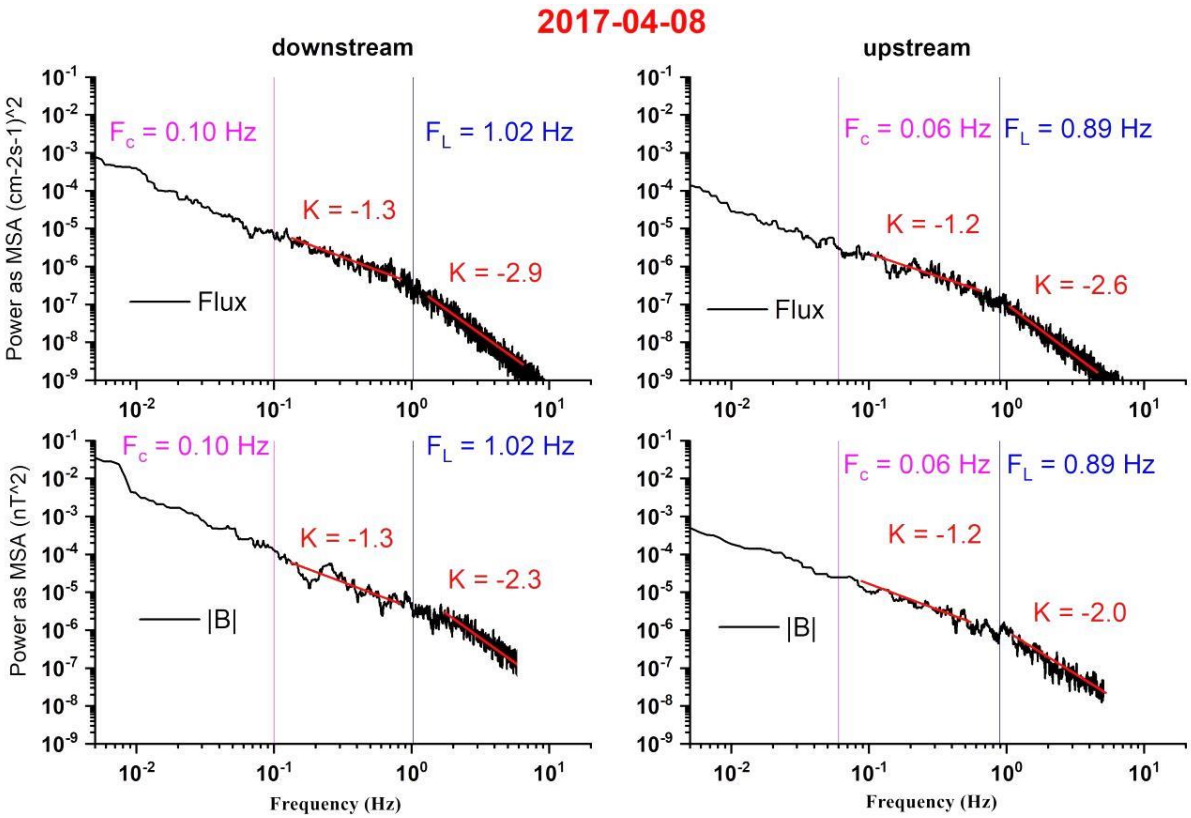

Figure 6. Fluctuation spectra of plasma flux (top panels) and IMF (bottom panels) for a reverse shock in downstream (left) and upstream (right) regions: F_C is the gyrofrequency, F_L is the inertial frequency; K values are given for the MHD and transition spectral regions

the wave front for forward and reverse IP shocks also have similar features, yet the statistics on reverse IP shocks were not enough to cover all the intervals. The magnetosonic Mach number M_{ms} for reverse IS also turned out to be lower on average than for the forward ones, which is consistent with the conclusions about a smaller velocity jump at the fronts of reverse IS, drawn on the basis of Figure 4.

2.2. Power spectra of fluctuations

Figure 6 exhibits power spectra of SW plasma flux and IMF magnitude fluctuations for the reverse IP shocks recorded on April 08, 2017. The spectra are presented for downstream and upstream SW regions (the order is explained by the relative position of these regions in the plot of the time variation in the parameters). The frequencies corresponding to proton gyroradius (F_C) and inertial length (F_L) are indicated.

An increase in the power of fluctuations can be seen during the transition to the downstream region, which agrees to both theoretical concepts and previous works [Rakhmanova et al., 2017]. The F_L frequency increases behind the front of this reverse IP shocks, although not as much as in the case of a fast forward shock [Sapunova et al., 2024]: a density increase in the downstream region is partially compensated by a decrease in the transport plasma flux velocity. From expression (1), F_L would be expected to be lower since the velocity enters (1) to the first power; and the density, to the 1/2 power. Nonetheless, a decrease in the transport velocity is generally ~10–20 % of that in the upstream region, whereas the density can increase significantly.

The spectrum slope coefficient K on the MHD scale is almost unchanged: –1.2 before and –1.3 after the shock front. The K values for the magnetic field and for the plasma flux are close. At the same time, in the transition part the spectra of the magnetic field (K varies from –2.0 to –2.3) and the plasma flux (K varies from –2.6 to –2.9) become somewhat steeper.

We have processed 55 fast forward and 14 fast reverse IP shocks. Using the data, we have constructed histograms of the frequency of spectrum breaks for SW plasma flux and IMF fluctuations.

2.3. Statistics on variations in the slope of fluctuation power spectra

Figure 7 presents the statistics on variations in coefficients of the slope of power spectrum for fast forward IP shocks. Similar studies have already been carried out by some authors [Pitňa et al., 2021; Zhao et al., 2021; Šafránková et al., 2015, 2016] and we provide the statistics for completeness. The spectrum is splitted into two parts by at least two different methods — according to the calculated frequency and by fitting the slope using the least square method. Here, we adopt the first method.

For the magnetic field, we can observe that in the MHD part of the spectrum, the slope may be steeper in the upstream region. This observation agrees with the results obtained in [Rakhmanova et al., 2017]. We observe the same effect for the slope of the power spectrum of plasma flux fluctuations. In the transition region, the average slope of the spectrum is much smaller

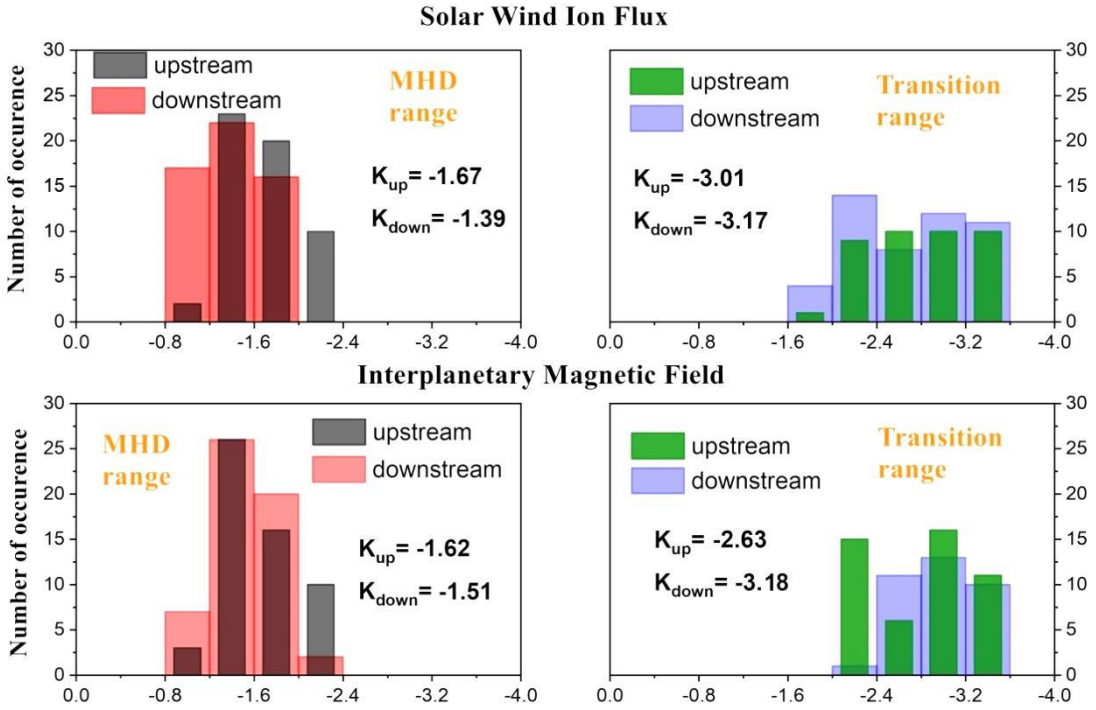

Figure 7. Histograms of coefficients of slopes of fluctuation spectra of the plasma flux (top row) and the magnetic field magnitude (bottom row) for forward IP shocks: left panels show MHD-part of the spectrum; right panels, the transition part of the spectrum; black and green colors denote data for the SW upstream region; red and blue, for the downstream one

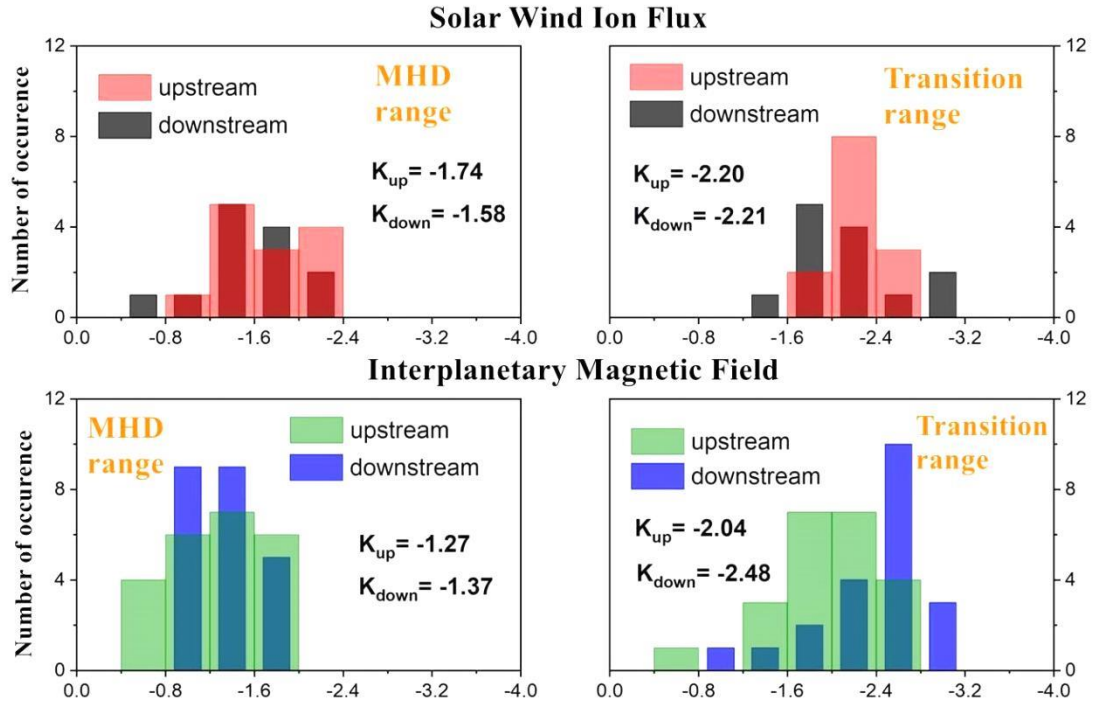

Figure 8. Histograms of the coefficients of slopes of fluctuation spectra of the plasma flux (top row) and the magnetic field magnitude (bottom row) for reverse IP shocks: left panels — MHD part of the spectrum, right panels — the transition part of the spectrum; black and green colors denote data for the SW upstream region; red and blue, for the downstream one

than in the MHD region, which is also consistent with the results of previous works. Note that the slope of the power spectrum of IMF fluctuations increases more strongly than for the SW plasma flux.

Figure 8 presents histograms of coefficients of the slope of the power spectrum of plasma flux and IMF fluctuations for reverse IP shocks.

For both the plasma flux and the magnetic field magnitude, the spectrum slope in the transition region is noticeably steeper than in the MHD region, by about 0.5–0.7. The maximum difference is recorded for the magnetic field spectrum in the downstream region — more than 1.1.

When comparing the regions before and after the IP shock front, noteworthy is a relatively small difference between the slope coefficients in the MHD part of the spectrum: the difference for the plasma flux was 0.16; and for the magnetic field magnitude, 0.1. In this case, the distributions are similar, although the magnetic field magnitude in the upstream region features slightly smaller absolute values of K for this part of the spectrum; and for the flux, slightly larger absolute values of K than in the downstream region.

The situation seems somewhat different in the transition region of the spectrum. The mean coefficient of the slope of the flux fluctuation spectrum is almost the same for the downstream and upstream regions. Yet, the distributions differ significantly in shape — behind the front of the reverse shock, the range of values is wider (from –1.2 to –3.2), and the maximum is slightly shifted. In the upstream region, the range is narrower (from –1.6 to –2.8). The histogram of the coefficient of the slope of the magnetic field spectrum shows even more serious differences. Along with the obvious variation in mean K (from –2.04 to –2.48), the maximum of the distribution is clearly shifted to a steeper part of the spectrum. Such a difference between the spectra of the flux and the magnetic field, in addition to physical reasons, might have been caused by the small statistical sample and technical differences in the instruments (the maximum measured frequency for the magnetic field from WIND data is 5.5 Hz; and for the plasma flux from BMSW data is 16 Hz). This issue requires further research.

3. DISCUSSIONS AND CONCLUSIONS

Using SPEKTR-R BMSW and WIND MFI magnetometer data, we have identified frequencies of breaks of power spectra of fluctuations in the total SW plasma flux and the magnetic field before and after the front of a reverse shock. We have calculated coefficients of the slope in the MHD and transition regions of the spectrum.

For the reverse shock, the frequency of the spectrum breaks ranged from 0.53 to 1.31 Hz in the downstream region and from 0.40 to 1.11 Hz in the upstream region. The means of this frequency were 0.94 and 0.75 Hz respectively. The frequency in the downstream region increases due to an increase in density behind the front of the reverse shock.

The study of variations in the slope of different spectral regions for the reverse shock gave a somewhat ambiguous result. The expected pattern was obtained for the interplanetary magnetic field, although with a smaller change in the slope coefficient during the transition to the downstream region — the spectrum becoms steeper in the transition region, but retains its shape in the MHD region. For the plasma flux, it can be seen behind the front of the reverse shock that the MHD region of the spectrum becomes slightly flatter. Yet, the effect is not so significant that we can certainly talk about its physical cause. It is also possible that this effect occurs due to insufficient statistics on fast reverse shocks.

At the same time, the transition region of the fluctuation spectrum has a much steeper slope than the MHD region, which was absolutely expected. This change when the shock is crossed can either increase or decrease, depending on the event. The means of K suggest that for the magnetic field the spectrum becomes much steeper than for the plasma flux. In some cases, the transition region of the power spectrum in the downstream region became flatter, which was also shown for forward IP shocks [Šafránková et al., 2015].

In the future, in-depth study of individual events is planned, which will help clarifying the criteria according to which it would be worthwhile to divide the statistics, starting with classifying parameters and frequencies of spectrum break.

The work was financially supported by RSF (Grant No. 22-12-00227).

REFERENCES

Bruno R., Carbone V. The solar wind as a turbulence laboratory. *Living Rev. Solar Phys.* 2013, vol. 10, no. 2. DOI: 10.12942/lrsp-2013-2.

Howes G.G., Cowley S.C., Dorland W., Hammett G.W., Quataert E., Schekochihin A.A. A model of turbulence in magnetized plasmas: Implications for the dissipation range in the solar wind. *Geophys. Res.* 2008, vol. 113. DOI: 10.48550/arXiv.0707.3147.

Kolmogorov A.N. A refinement of previous hypotheses concerning the local structure of turbulence in a viscous incompressible fluid at high Reynolds number. *J. Fluid Mech*. 1962, vol. 13, pp. 82–85. DOI: 10.1017/S0022112062000518.

Leamon R.J., Matthaeus W.H., Smith C.W., Zank G.P., Mullan D.J., Oughton S. MHD-driven kinetic dissipation in the solar wind and corona. *Astrophys. J.* 2000, vol. 537, no. 2, pp. 1054–1062. DOI: 10.1086/309059.

Matthaeus W.H., Weygand J.M., Dasso S. Ensemble space-time correlation of plasma turbulence in the solar wind. *Phys. Rev. Lett*. 2016, vol. 116, no. 245101. DOI: 10.1103/PhysRevLett.116.245101.

Oliveira D.M. Magnetohydrodynamic shocks in the interplanetary space: A theoretical review. *Braz. J Phys.* 2017, vol. 47, pp. 81–95. DOI: 10.1007/s13538-016-0472-x.

Park B., Pitňa A., Šafránková J., Němeček Z., Krupařová O., Krupař V., Zhao L., Silwal A. Change of spectral properties of magnetic field fluctuations across different types of interplanetary shocks. *Astrophys. J. Lett.* 2023, vol. 954, no. 2. DOI: 10.3847/2041-8213/acf4ff.

Pitňa A., Šafránková J., Němeček Z., Ďurovcová T., Kis A. Turbulence upstream and downstream of interplanetary shocks. *Front. Phys.* 2021, vol. 8, no. 626768. DOI: 10.3389/fphy.2020.626768.

Rakhmanova L.S., Riazantseva M.O., Borodkova N.L., Sapunova O.V., Zastenker G.N. Impact of interplanetary shock on parameters of plasma turbulence in the Earth's magnetosheath. *Geomagnetism and Aeronomy*. 2017, vol. 57, no. 6, pp. 664–671. DOI: 10.1134/S00 16793217060093.

Šafránková J., Němeček Z., Přech L., Zastenker G., Čermák I., Chesalin L., et al. Fast solar wind monitor (BMSW): Description and first results. *Space Sci. Rev.* 2013, vol. 175 (1-4), pp. 165–182. DOI: 10.1007/s11214-013-9979-4.

Šafránková J., Němeček Z., Němec F., Přech L., Pitňa A., Chen C.H.K., Zastenker G.N. Solar wind density spectra around the ion spectral break. *Astrophys. J*. 2015, vol. 803, p. 107. DOI: 10.1088/0004-637X/803/2/107.

Šafránková J., Němeček Z., Němec F., Přech L., Chen C.H.K., Zastenker G.N. Power spectral density of fluctuations of bulk and thermal speeds in the solar wind. *Astrophys. J.* 2016, vol. 825, p. 121. DOI: 10.3847/ 0004-637X/825/2/121.

Sapunova O.V., Borodkova N.L., Yermolaev Yu.I., Zastenker G.N. Spectra of fluctuations of solar wind plasma parameters near a shock wave. *Cosmic Res*. 2024, vol. 62, no.1, pp. 1–9. DOI: 10.1134/S0010952523700843.

Schekochihin A.A., Cowley S.C., Dorland W., Hammett G.W., Howes G.G., Quataert E., Tatsuno T. Astrophysical gyrokinetics: kinetic and fluid turbulent cascades in magnetized weakly collisional plasmas. *Astrophys. J. Suppl. Ser*. 2009, vol. 182, no. 1, pp. 310–377. DOI: 10.1088/0067-0049/182/1/310.

Smith C.W., Mullan D.J., Ness N.F., Ruth M.S., John S. Day the solar wind almost disappeared: Magnetic field fluctuations, wave refraction and dissipation. *Geophys. Res*. 2001, vol. 106, pp. 18625–18634. DOI: 10.1029/2001JA000022.

Zastenker G.N., Safrankova J., Nemecek Z., Prech L., Cermak I., Vaverka I., Komarek A., Voita J., et al. Fast measurements of parameters of the solar wind using the BMSW instrument. *Cosmic Res.* 2013, vol. 51, p. 78. DOI: 10.1134/S00 10952513020081.

Zhao L.-L., Zank G.P., He J.S., Telloni D., Hu Q., Li G., Nakanotani M., Adhikari L., et al. Turbulence and wave transmission at an ICME-driven shock observed by the solar orbiter and wind. *Astron. and Astrophys.* 2021, vol. 656, no. A3. DOI: 10.1051/0004-6361/202140450.

This paper is based on material presented at the 19th Annual Conference on Plasma Physics in the Solar System, February 5–9, 2024, IKI RAS, Moscow.

Original Russian version: Sapunova O.V., Borodkova N.L., Zastenker G.N., published in Solnechno-zemnaya fizika. 2024. Vol. 10. No. 3. P. 62–69. DOI: 10.12737/szf-103202407.

How to cite this article

Sapunova O.V., Borodkova N.L., Zastenker G.N. Spectral properties of solar wind plasma flux and magnetic field fluctuations across fast reverse interplanetary shocks. *Solar-Terrestrial Physics*. 2024. Vol. 10. Iss. 3. P. 58–65. DOI: 10.12737/stp-103202407.